Advanced Electro-Oxidation with Boron-Doped Diamond for Acetaminophen Removal from Real Wastewater in a Microfluidic Reactor: Kinetics and Mass-Transfer Studies

Emmanuel Mousset, Marta Puce, Marie-Noëlle Pons

Advanced electro-oxidation with boron-doped diamond for acetaminophen removal from real wastewater in a microfluidic reactor – Kinetics and mass transfer studies

Dr. Emmanuel Mousset,[*][a] Marta Puce,[a] Dr. Marie-Noëlle Pons[a]

[a] Laboratoire Réactions et Génie des Procédés, Université de Lorraine, CNRS, LRGP, F-54000 Nancy, France.

Accepted version

CHEMELECTROCHEM

(Special issue "Trends in Synthetic Diamond for Electrochemical Applications")

*Correspondence to:

Emmanuel MOUSSET: emmanuel.mousset@univ-lorraine.fr; phone number: +33 (0)3 72 74 37 44

TABLE OF CONTENTS

Boron-doped diamond (BDD) anode is implemented in an electrochemical microfluidic cell for electrocatalytic treatment of acetaminophen in synthetic and reclaimed wastewater. An optimal interelectrode distance could be determined at optimal mass transfer and optimal decay rate constant. The low conductivity reclaimed wastewater could be treated with the same range of energy requirement than in synthetic solution. The energy efficiency could be maximized with short interelectrode gap in order to minimize the negative impact of the low conductivity of solutions.

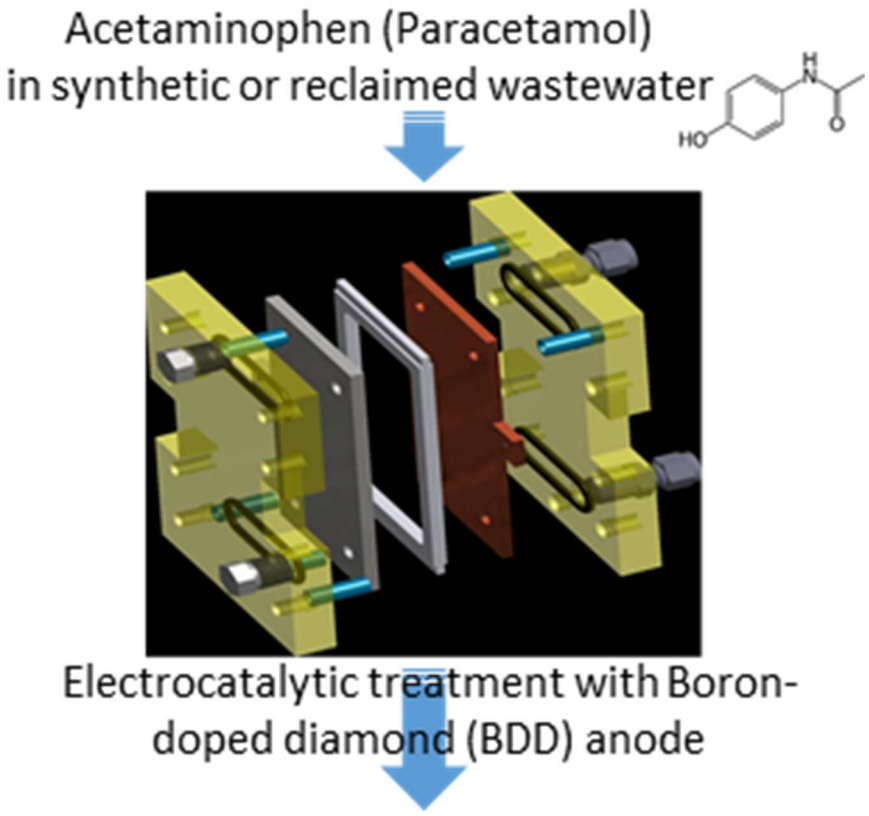

ABSTRACT

The removal of hazardous organic micropollutants in municipal wastewater treatment plants (WWTP) has become a common concern for public decision-makers and stakeholders. An advanced electro-oxidation with boron-doped diamond (BDD) anode material is proposed to remove acetaminophen as a representative micropollutant in synthetic solution. A customized microfluidic reactor was run in batch mode, and the main operating parameters (i.e., current density, interelectrode distance and solution conductivity) were optimized by minimizing the energy requirement. An optimal current density of 4 mA cm^{-2} and an optimal interelectrode distance of 500 µm were newly obtained and explained. Mass transport limitation was observed at lower gaps, with a 3.4-fold decrease in the mass transfer coefficient from 500 µm to 50 µm intervals. In addition, the kinetics of degradation decreased dramatically after a certain electrolysis time. This was attributed to the increase in gas bubble production with treatment time. An increase in the solution conductivity from 0.23 mS cm^{-1} to 2.0 mS cm^{-1} increased the degradation rate efficiency by 2-fold and decreased the specific energy from 0.88 to 0.17 kWh g^{-1} at 85% acetaminophen decay yield. The influence of a real matrix from low-conductivity reclaimed WWTP (1 mS cm^{-1}) highlighted slightly lower kinetics of degradation, but similar energy efficiency until 60% of pollutant degradation and higher energy efficiency than in conventional macro-reactors.

1. Introduction

Electrochemical processes have been widely studied for the last two decades to answer the challenge of wastewater treatment contaminated by hazardous biorecalcitrant pollutants that are barely removed in conventional wastewater treatment plants (WWTP).[1–6] Electrochemical advanced oxidation processes (EAOP) offer the advantages of continuously *in situ* generated strong oxidizing agents, such as hydroxyl radicals (•OH) ($E°$ = 2.80 V / standard hydrogen electrode (SHE)) responsible for the degradation and mineralization of organic pollution.[7,8] Boron-doped diamond (BDD) anodes have been developed to promote oxidation by heterogeneous catalysis.[9–12] The high oxygen (O_2) evolution overvoltage (approximately 2.3 V / SHE) allows for the generation of physisorbed •OH at the BDD surface from water oxidation (Eq. 1):[9]

$$BDD + H_2O \rightarrow BDD(^{\bullet}OH) + H^+ + e^- \quad (1)$$

This so-called anodic oxidation or advanced electro-oxidation process has been widely developed since the early 2000s as a promising EAOP.[13,14] No pH adjustment is required, and no chemicals are needed except for the supporting electrolyte for the low-conductivity solution. Effluents at the outlet of municipal WWTP exhibit conductivity of approximately 1 mS cm^{-1}, which is too low to efficiently drive the electric current in conventional electrolytic systems. The addition of electrolyte would constitute an external contamination, since the salts – usually sulfated or chlorinated compounds – need to be removed after the electrolytic treatment. Electrochemical microfluidic reactors have therefore been proposed to address this issue by implementing a very short interelectrode distance (50-500 µm).[15–17] This process allows for minimizing the ohmic drop and then the cell resistance, i.e., the conductivity requirement. In the meantime, the cell potential is reduced, which permits a decrease in the energy consumption of the cell,[18] another typical drawback in conventional EAOP technologies. A further advantage is the transfer intensification, which increases the oxygen redox cycle and iron redox cycle in undivided microcells. The process then accentuates the rate of H_2O_2 production and Fe^{2+} regeneration in the electro-Fenton system.[17]

Charge and mass transfer are primordial phenomena to take into account in such reactors, especially when heterogeneous catalysis is involved with the use of a BDD anode.[19] This study investigates their importance in a BDD-microfluidic reactor for the degradation of acetaminophen as a representative of pharmaceuticals in wastewater (Fig. 1). Also known as paracetamol, it is a widely prescribed analgesic and anti-pyretic drug that has been detected in groundwater[20] and surface water[21,22] in concentrations up to 65 µg L^{-1}[23]. Even at low concentrations, acetaminophen can cause damage to aquatic life and human health.[24] The influence of main parameters, such as current density, interelectrode gap and solution conductivity, is studied, and the factors are optimized by considering decay rates, mass transfer and specific energy requirements.

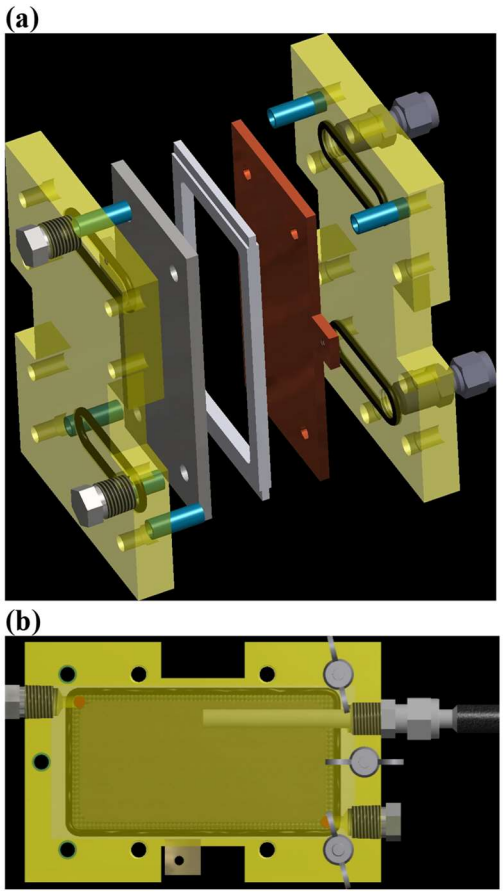

Fig. 1. Scheme of the micro-fluidic electrochemical reactor developed in the laboratory. (a) Exploded view of the complete cell and (b) view of the graphite felt cathode compartment.

2. Results and discussion

2.1. Influence of current density on degradation efficiency

The current density is an important parameter to optimize electrochemical processes since it controls the kinetics of electrochemical reactions.

The applied current density (J_{appl}) was varied from 2 to 12 mA cm^{-2}, and the impact on the kinetics of acetaminophen degradation is plotted in Fig. 2a. A pseudo-first-order kinetic model was considered as a first approach for apparent rate constant determination as usually proposed in the literature.[25] The correlation coefficients (R^2) values varied from 0.986 to 0.991, which is close to 1 and validates the model assumption.

An 8-fold increase in the degradation rate was observed from 2 to 4 mA cm^{-2}, while a plateau from 4 to 9 mA cm^{-2} was observed (k_{app} = 0.054 ± 0.002 min^{-1}) before a decrease in the degradation rate constant at 12 mA cm^{-2} (k_{app} = 0.018 min^{-1}) (Fig. 2a). At higher current density values, the secondary reaction, such as the O_2 evolution reaction at the anode, becomes increasingly important according to Eq. 2, being in competition with the production of $^{\bullet}OH$ (Eq. 1), while the hydrogen evolution reaction occurs at cathode surface (Eq. 3).[9,26,27]

$$2H_2O \rightarrow O_{2(g)} + 4H^+ + 4e^- \quad (2)$$

$$2H^+ + 2e^- \rightarrow 2H_{2(g)} \quad (3)$$

To better assess the oxidation performance in BDD cell system, the electroactivity of acetaminophen has been previously tested in a platinum (Pt) anode / graphite cathode system immersed in 157 mg L^{-1} of acetaminophen synthetic solution.[28] Pt is an active anode having lower O_2 evolution overvoltage (1.7-1.9 V / SHE) than BDD.[4] $^{\bullet}OH$ are therefore chemisorbed at Pt surface indicating that $^{\bullet}OH$ are barely available for oxidation. Thus, direct electro-oxidation mainly occurs in presence of Pt anode. At a current density of 100 mA cm^{-2}, a TOC decrease of 20% was noticed after applying a specific charge of 18 Ah L^{-1} against 99% of TOC removal with BDD anode.[28] This previous work highlight the ability of acetaminophen to be oxidized by direct electron transfer though the use of BDD clearly depicted its superiority by involvement of advanced oxidation. Acetaminophen's molecular structure presents

unsaturated bonds, especially in its aromatic ring. •OH reacts particularly very quickly with double C=C bonds, which makes advanced oxidation mechanism more selective and efficient as compared to direct oxidation mechanism.

Another recent study confirms the electroactivity of acetaminophen using graphite anode that is an active anode such as Pt.[23] Upon these results, it is important to emphasize that the degradation and mineralization efficiencies presented in this paper are also due to direct electro-oxidation, in a lesser extent than advanced oxidation.

The specific energy consumption ($E_{specific}$), expressed in kWh per gram of pollutant removed (kWh g^{-1}) and calculated according to Eq. 4,[1] is a decisive aspect to take into account because it represents an important part of the operating costs.[29]

$$E_{specific} = \frac{E_{cell} I t}{V_s (C_0 - C)} \quad (4)$$

where E_{cell} is the average cell voltage (V), I is the applied current intensity (A), t is the electrolysis time (h), V_s is the solution volume (L), and C_0 and C are the initial concentration and the concentration at time t of acetaminophen (mg L^{-1}), respectively.

The $E_{specific}$ values are represented as a function of the acetaminophen degradation yield in Fig. 1b for different J_{appl} values. J_{appl} of 9 and 12 mA cm^{-2} clearly appeared as high energy-demanding conditions, regardless of the disappearance percentage. 4 mA cm^{-2} required the lowest specific energy (0.11 – 0.50 kWh g^{-1}) for up to 83% of decay, while 3 mA cm^{-2} offered better energy efficiency (0.19 – 0.31 kWh g^{-1}) for 83% to 87% of acetaminophen degradation. Knowing that the kinetics rate of degradation was 1.6-fold lower with 3 mA cm^{-2} conditions compared with 4 mA cm^{-2}, the latter current density seems optimal and has been selected for further optimization.

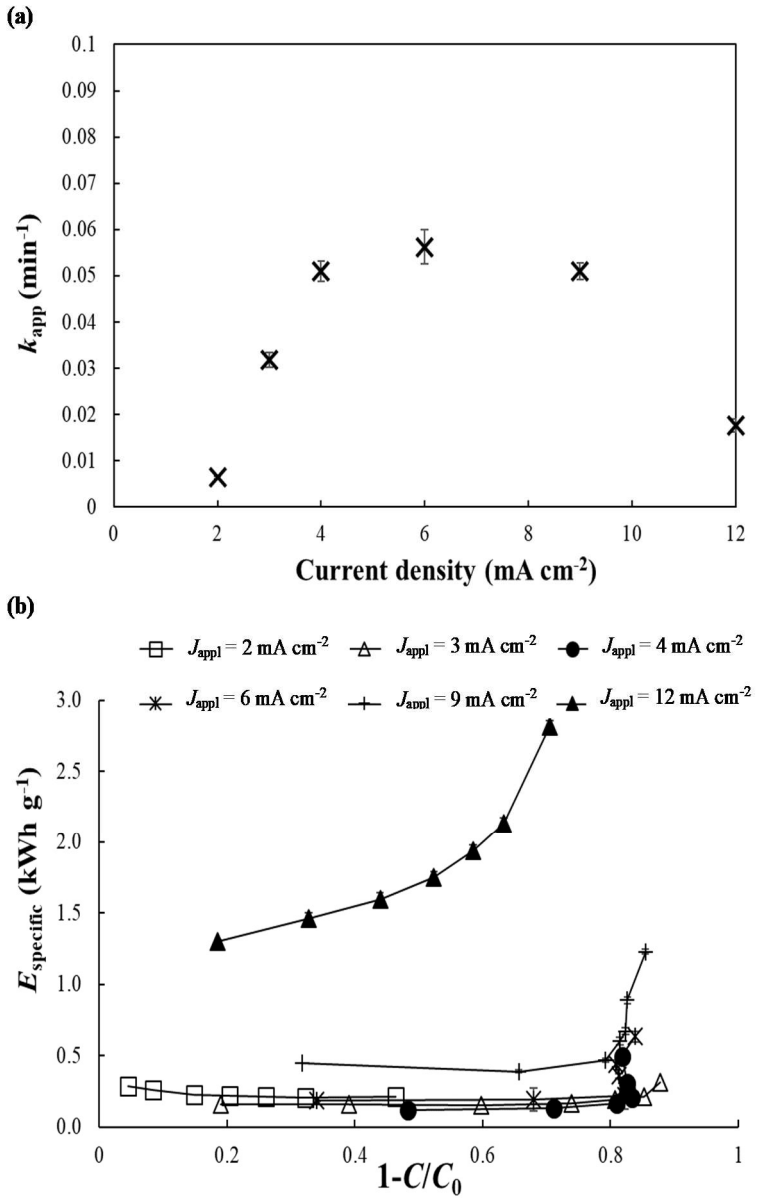

Fig. 2. Influence of current density on: (a) decay rate constant in a microfluidic electrochemical reactor, (b) specific energy efficiency as function of the pollutant degradation yield. Operating conditions: $[acetaminophen]_0$ = 0.1 mM, cathode = carbon felt, anode = BDD, interelectrode distance = 50 μm, $[Na_2SO_4]$ = 10 mM, pH = 3.

2.2. Influence of interelectrode distance

2.2.1. Mass transfer determination

The acetaminophen concentration decay curve is represented in Fig. 3 for a 250 µm interelectrode distance. It appears that there are two trends during electrolysis, i.e., a linear trend at the beginning of the treatment followed by an exponential trend until the end of the electrolysis, as described previously by Comninellis' team.[13,30] The first trend can be assimilated to a zero-order kinetic model until J_{appl} reaches the limiting current density (J_{lim}) value. Then, the diffusion becomes the rate-limiting step, and J_{appl} is higher than J_{lim}.

The electrolytic systems are mainly governed by two transfers: (i) the charge transfer at the electrode surface during the electrochemical reaction and (ii) the mass transfer of the target pollutant from the bulk solution to the electrode surface and from the electrode to the bulk.[19,31] Thus, at $J_{appl} < J_{lim}$ (zero-order model), the process is under charge transfer control, while at $J_{appl} > J_{lim}$ (pseudo-first-order model), it is under mass transfer control. The time at which the kinetic order switches is named the critical time (t_{cr}).[13,30] When $t = t_{cr}$, $J_{appl} = J_{lim}$, and J_{lim} (A m^{-2}) can be defined as follows (Eq. 5):[13,30,32]

$$J_{lim} = nFk_mC_{lim} \quad (5)$$

where n is the number of electrons exchanged, F is the Faraday constant (96485 C mol^{-1}), k_m is the mass transfer coefficient (m s^{-1}) and C_{lim} is the concentration (mol m^{-3}) of the target compound (acetaminophen in this study) at $t = t_{cr}$.

The number of electrons exchanged during the partial electrochemical combustion of acetaminophen ($C_8H_9O_2N$) at the BDD anode can be estimated by considering benzoquinone as the first main by-products,[33,34] according to the following reaction (Eq. 6):

$$C_8H_9O_2N + 2/3\ H_2O \rightarrow 4/3\ C_6H_4O_2 + NH_3 + 2\ H^+ + 2\ e^- \quad (6)$$

It can be concluded that $n = 2$ for acetaminophen degradation. From Fig. 3, the C_{lim} can be deduced from $(C/C_0)_{lim}$ (C_0 is the initial concentration of acetaminophen) at $t = t_{cr}$ (Table 1), and

k_m can then be calculated for each interelectrode gap experiment using Eq. 5 for $J_{appl} = J_{lim}$ = 40 A m^{-2}. Table 1 gives t_{cr} and $(C/C_0)_{lim}$ values for each interelectrode distance. It was shown that $(C/C_0)_{lim}$ increases from 500 µm to 1000 µm and to 50 µm because the mass transfer become the limiting factor very quickly as compared to charge transfer in these conditions.

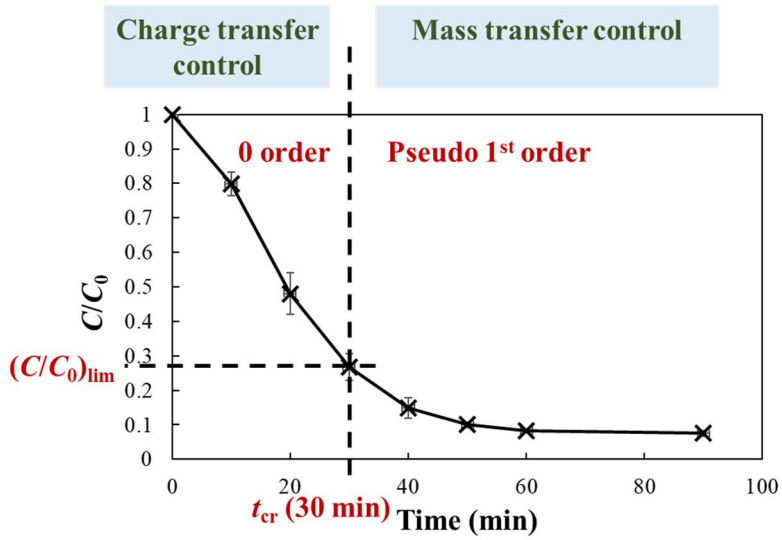

Fig. 3. Acetaminophen decay in a microfluidic electrochemical reactor. Operating conditions: $[acetaminophen]_0$ = 0.1 mM, cathode = carbon felt, anode = BDD, J_{appl} = 4 mA cm^{-2}, interelectrode distance = 250 µm, $[Na_2SO_4]$ = 10 mM, pH = 3.

Table 1. t_{cr} and $(C/C_0)_{lim}$ values for each interelectrode distance.

Interelectrode distance (µm)	t_{cr} (min)	$(C/C_0)_{lim}$
50	10	0.52
250	30	0.26
500	35	0.16
1000	15	0.48

2.2.2. Effect of electrode distance on mass transfer and energy efficiency

The mass transfer coefficients calculated from section 2.2.1 have been plotted as a function of the different interelectrode distances (50, 250, 500, 1000 µm) in Fig. 4a. A maximum acetaminophen mass transfer coefficient (12.6 × 10^{-3} m s^{-1}) was reached at 500 µm, while the mass transfer coefficients varied from 3.9 × 10^{-3} m s^{-1} (50 µm) to 7.8 × 10^{-3} m s^{-1} (250 µm) at

shorter distances. The change of mass transfer coefficients with the interelectrode distance corroborated previous studies.[18,35] The existence of an optimum in this work provides new insight, as it could explain the existence of an optimal degradation efficiency value obtained when varying the interelectrode distance in previous studies dealing with electrochemical microreactors for wastewater treatment.[15,36] This feature could be attributed to the transfer limitation by gas bubbles[37] through the formation of $O_{2(g)}$ at the anode (Eq. 2) and $H_{2(g)}$ at the cathode (Eq. 3) at a low interelectrode gap (50 and 250 µm).

It has been previously emphasized that the current density increases at the edge of a parallelepiped flow-by cell with the contraction of interelectrode distance.[37] As the current density increases the bubble size,[37] it has an impact on the mass transfer at small gaps. Nevertheless, the maximal k_m value was higher than in a flow-by reactor with gaps of 1000 µm and 5000 µm, giving k_m values of 1.5×10^{-5} m s^{-1} and 7×10^{-6} m s^{-1} respectively, at 5 L min^{-1},[35] 830 to 1785 times lower than in our study. The difference is even higher compared with stirred tank reactor configurations ($k_m = 5.9 \times 10^{-6}$ m s^{-1}).[38–40] It remains important to highlight that our k_m calculation consider the targeted pollutant transfer towards anode for its subsequent degradation and does not take into account the ferrocyanide representative compound usually employed for mass transfer characterization[32]. The difference of method could partly explain the difference of k_m range.

In parallel to the hydrodynamic aspects, the kinetic rate constants (k_{app}) of acetaminophen degradation assuming a pseudo-first-order model under mass transfer control have been plotted in Fig. 4b. R^2 values varied from 0.975 to 0.995 – close to 1 – indicating a good fit between the model and the experimental data. The k_{app} values decreased from 0.058 min^{-1} to 0.033 min^{-1} with the interelectrode distance varying from 50 µm to 1000 µm. No optimal k_{app} value was noticed in this condition, which is also noted in the literature.[15] However, the kinetics rate decreased towards the end of electrolysis, especially at 50 µm and 250 µm interelectrode distances, when looking at acetaminophen concentration decay in Fig. 4c. This phenomenon could be ascribed to the increase of bubble formation with electrolysis time. Indeed, current

efficiency tends to decrease after a certain electrolysis time,[19,41] along with the increased occurrence of secondary reactions such as in Eqs. 2 and 3. This feature is also highlighted in energy considerations, as depicted in Fig. 4d. At 50% to 80% of decay, the energy requirements varied from 0.11 to 0.17 kWh g^{-1}, while they increased dramatically at higher acetaminophen degradation percentages at a 50 μm interelectrode distance. In the range of 50-80% disappearance, the energy consumption equaled 0.17 kWh g^{-1} at 500 μm of the interelectrode gap and increased from 0.18 to 0.36 kWh g^{-1} for degradation percentages of 84% to 94%. At the highest oxidative degradation yields, 500 μm became the optimal interelectrode distance. A distance of 1000 μm – corresponding to a more conventional gap – clearly showed higher specific energy consumption, varying from 0.18 to 0.56 kWh g^{-1} with 30% to 83% decay yield, respectively, compared to the shorter intervals. It emphasizes the benefit of decreasing the distance on the energy efficiency due to the decrease of cell potential. A cell voltage of 4.1 V was measured at 1000 μm against 2.9 V at 500 μm, corresponding to a 30% decrease in cell voltage. This confirmed the trend obtained in a previous work, with a decrease of cell potential of approximately 1 V when decreasing the interelectrode distance from 4000 μm to 120 μm.[15]

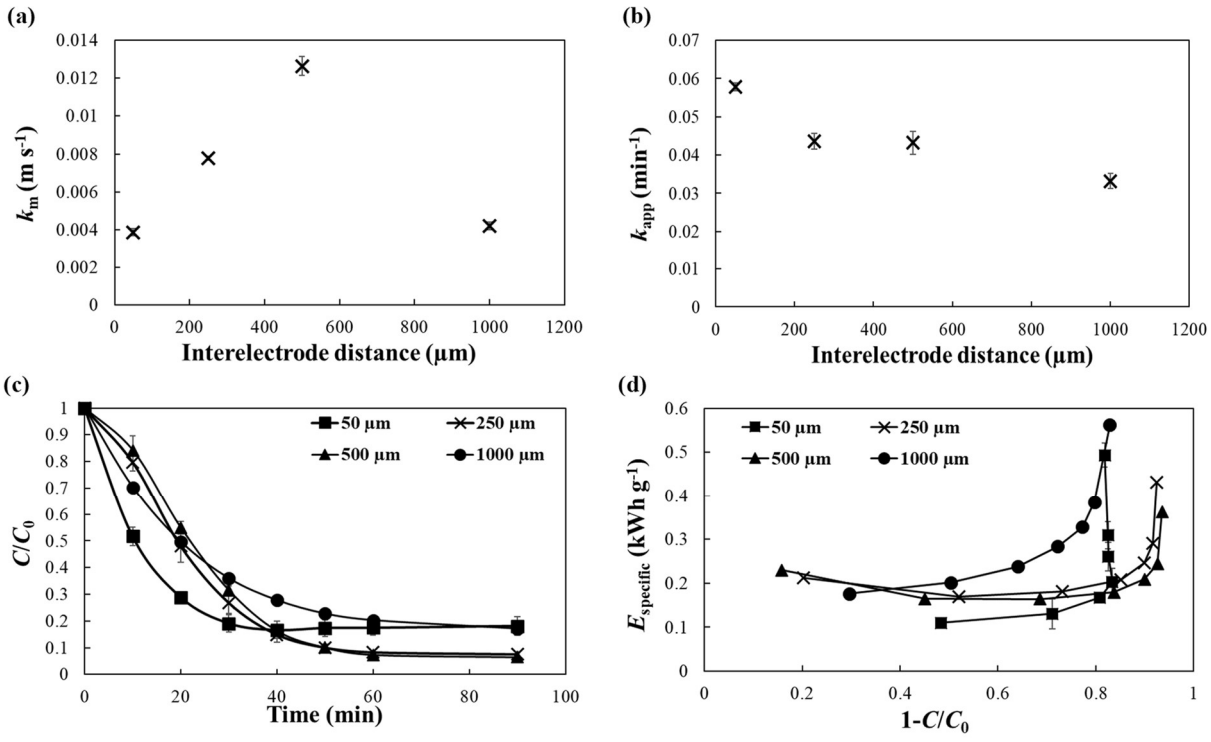

Fig. 4. Influence of interelectrode distance on (a) mass transfer coefficient, (b) apparent rate constants for acetaminophen degradation, (c) acetaminophen concentration decay and (d) specific energy consumption as a function of the pollutant degradation yield. Operating conditions: $[acetaminophen]_0$ = 0.1 mM, cathode = carbon felt, anode = BDD, J_{appl} = 4 mA cm^{-2}, $[Na_2SO_4]$ = 10 mM, pH = 3.

2.3. Influence of solution conductivity

The conductivity is another valuable parameter to investigate when the addition of supporting electrolyte needs to be avoided, especially in the context of wastewater treatment.[42] Fig. 5a displays the evolution of k_{app} for acetaminophen degradation as a function of the conductivity of the solution when varying the electrolyte concentration ($[Na_2SO_4]$) from 0 to 10 mM. A pseudo-first-order kinetic model was assumed to determine the rate constants, and the model fit the experimental data well, with R^2 varying from 0.988 to 0.994. No acetaminophen degradation occurred with ultrapure water in the absence of electrolyte because it could not overcome the cell resistance that remained in solution, even at microdistances.

Moreover, a nonlinear increase of k_{app} as a function of conductivity was revealed. k_{app} increased from 0.026 min^{-1} to 0.040 min^{-1} and 0.051 min^{-1} when the solution conductivity increased from 0.23 mS cm^{-1} to 0.86 mS cm^{-1} and 2.0 mS cm^{-1}. One reason could be that an increase in salinity leads to an increase in the importance of the mediated oxidation mechanism through the oxidation of sulfate ions from the electrolyte (Na_2SO_4) into sulfate radical ($SO_4^{\bullet-}$) at the BDD anode surface and persulfate ($S_2O_8^{2-}$) in bulk solution.[43,44] These species are strong oxidizing agents that take part in the whole oxidation process.[2]

The influence of solution conductivity on the specific energy is depicted in Fig. 5b. An energy increase from 0.31 to 0.88 kWh g^{-1} was required for an acetaminophen decay yield varying from 26% to 85% at 0.23 mS cm^{-1}. In contrast, the energy requirements at 0.86 mS cm^{-1} and 2.0 mS cm^{-1} were lower. For instance, from 3.8 times (0.86 mS cm^{-1}) to 4.9 times (2.0 mS cm^{-1}), lower energy was needed to reach 85% of pollutant degradation. The increase in conductivity decreases the cell resistance and therefore the cell potential. Thus, an average

cell potential difference of 3.5 V was noticed between the experiments at 0.23 mS cm^{-1} and 2.0 mS cm^{-1}, which mainly explained the contrast of energy demand.

A solution conductivity is still required to drive the electric current, but it can be minimized in microfluidic cells compared to the range of electrolyte concentrations (50-100 mM) used in conventional reactor design. Sulfate- or chlorine-based electrolytes are widely employed in the literature.[45–49] Consequently, high concentrations of sulfate and chlorine ions are released after the electrolytic treatment and are not removed during electrolysis. Hazardous chlorinated transformation products can also be formed during electrolysis, such as organochlorinated compounds (e.g., trihalomethanes (THMs)) and inorganic species that tend to accumulate (chlorate (ClO_3^-) and perchlorate (ClO_4^-)).[42,50,51] Since a conductivity of 1 mS cm^{-1} corresponds to the average conductivity of the municipal WWTP outflow, the decrease of degradation efficiency compared to the addition of supporting electrolytes, such as Na_2SO_4 at 10 mM (2.0 mS cm^{-1}) or even higher concentrations, would be negligible considering the nonlinear trend observed in Fig. 5a. Thus, the gain that can be achieved by avoiding the addition of chemicals must be considered.

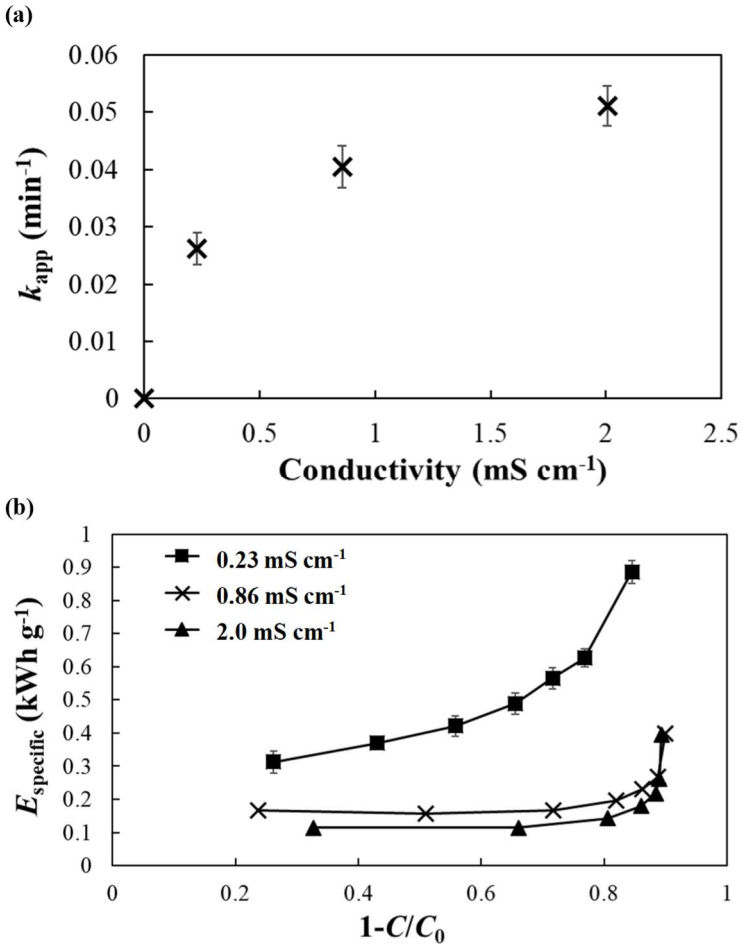

Fig. 5. Influence of conductivity on (a) pollutant decay rate constants and (b) specific energy consumption as a function of the pollutant degradation yield. Operating conditions: $[acetaminophen]_0$ = 0.1 mM, cathode = carbon felt, anode = BDD, interelectrode distance = 500 µm, J_{appl} = 4 mA cm^{-2}, no pH adjustment.

2.4. Influence of reclaimed municipal wastewater on degradation and mineralization of acetaminophen

The influence of reclaimed municipal wastewater on the process efficiency has been assessed. The physico-chemical properties of the real solution are presented in Table 2. The pH was circum-neutral (7.7) and the conductivity equal 0.86 mS cm^{-1}. The total organic carbon (TOC) was around 4.2 mg L^{-1}, which represented 7% of the total carbon present in wastewater. Inorganic carbon, i.e. bicarbonate (HCO_3^-) and carbonate (CO_3^{2-}) under the pH condition, was the major source of carbon (56.9 mg L^{-1}).

Table 2. Physico-chemical characteristics of the reclaimed municipal WWTP effluent.

Parameter	Value
pH	7.7
Conductivity (mS cm^{-1})	0.86
PO_4^{3-} (mg L^{-1})	0.634
NO_3^- (mg L^{-1})	3.80
NO_2^- (mg L^{-1})	0.120
SO_4^{2-} (mg L^{-1})	55.2
Cl^- (mg L^{-1})	103
NH_4^+ (mg L^{-1})	1.22
Total inorganic carbon (TIC) (mg-C L^{-1})	56.9
Total organic carbon (TOC) (mg-C L^{-1})	4.17
Total nitrogen (TN) (mg-N L^{-1})	0.69

The reclaimed wastewater was spiked by acetaminophen (0.1 mM) to evaluate the influence of the matrix on the degradation efficiency and the results are depicted in Fig. 6. The acetaminophen concentration decreased from 0.10 mM to 0.033 mM after 90 min of treatment, reaching 67% of decay yield (Fig. 6a). The degradation rate constant was 0.015 min^{-1} assuming a pseudo-first order model with a good correlation (R^2 = 0.990). The kinetics can be compared to the experiment at 4 mM of Na_2SO_4 in synthetic solution since the saline conditions are closed (0.86 mS cm^{-1}). Considering the difference of treated volume, i.e. 500 mL in real solutions against 200 mL in synthetic media, at equivalent residence time the decay rate constant was 3000 min^{-1} in real matrix compared to 3200 min^{-1} in synthetic solution. The efficiency was slightly affected with 6% of rate constant decrease in presence of real matrix. Bicarbonate are known to be good $^{\bullet}OH$ scavenger by reacting very quickly.[52] Considering the high inorganic carbon (IC) concentration compared to the total carbon content (70.7 mg-C L^{-1}) including acetaminophen (9.6 mg-C L^{-1}), the competition should not be negligible. This is corroborated by the 21% decrease of IC concentration during the 90 min of electrolysis.

The specific energy remains similar to synthetic solution until 60% of degradation with a quasi-constant value of 0.15 kWh g^{-1} (Fig. 6b). The energy requirement starts increasing at higher degradation yield with an energy of 0.22 kWh g^{-1} for 70% of decay.

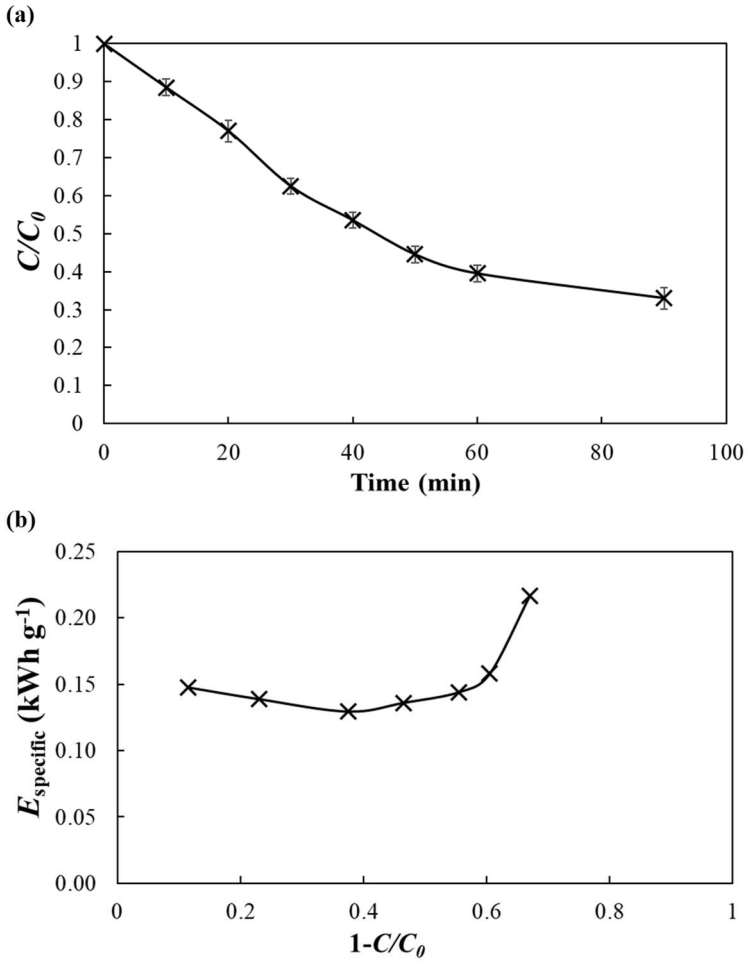

Fig. 6. Influence of reclaimed municipal wastewater on (a) acetaminophen degradation and (b) specific energy consumption as a function of the pollutant degradation yield. Operating conditions: $[acetaminophen]_0$ = 0.1 mM, cathode = carbon felt, anode = BDD, interelectrode distance = 500 µm, J_{appl} = 4 mA cm^{-2}, no pH adjustment.

The total organic carbon (TOC) has been monitored in order to take into account the global organic pollution, including the potential toxic organic by-products that could be produced.[25] The TOC removal of reclaimed wastewater spiked with acetaminophen (0.1 mM) is depicted in Fig. 7a. The TOC decreased from 13.7 mg-C L^{-1} to 0.37 mg-C L^{-1} in 4 h of treatment, leading to 87% of mineralization. Comparatively, an acetaminophen mineralization of 41% was noticed after 4 h of electrolysis of synthetic solution at 25°C with BDD cell implementing 30,000 µm of interelectrode gap with a treated volume of 100 mL.[34] Therefore, the mineralization yield was two times higher in our work even though our treated volume was 500 mL instead of 100 mL. Moreover, the applied conditions in the previous study led to an applied specific charge of 12

Ah L^{-1} against 1.6 Ah L^{-1}, 7.5 times higher than in the present work. The difference of efficiency could be attributed to the 60-fold shorter electrode distance involved that greatly enhance the mass transfer as above-mentioned.

The mineralization current efficiency (*MCE*) has been calculated according to Eq. 7:

$$MCE = \frac{\Delta(TOC)_{exp}}{\Delta(TOC)_{th}} \times 100 = \frac{(TOC_0 - TOC)nFV_S}{4.32\times10^7 mIt} \times 100 \quad (7)$$

where TOC_0 and *TOC* are the initial TOC concentration and the TOC concentration at time *t* (mg-C L^{-1}), respectively, and *m* is the number of carbon atoms of acetaminophen ($C_8H_9O_2N$) (*m* = 8).

The number of exchanged electron (*n*) has been determined using relation 8, considering complete electrochemical combustion of acetaminophen at the BDD anode:

$$C_8H_9O_2N + 14\ H_2O \rightarrow 8\ CO_2 + NH_3 + 34\ H^+ + 34\ e^- \quad (8)$$

The *MCE* values are displayed in Fig. 7b. An increase of *MCE* until 15.3% is noticed during the first hour of treatment while it decreases until 7.4% after 4 h of electrolysis. This trend is probably due to the more easily oxidizable aromatic intermediates as compared to the carboxylic acids such as oxalic and oxamic acids that are the end-products before CO_2 conversion.[34] A *MCE* of 9.7% was obtained by Brillas et al.[34] after 4 h of treatment. The slightly lower values of *MCE* in the present study could be explained by the presence of organic matter (OM) that represented around 30% of the TOC. This OM is in competition with the targeted pollutant, since it can also react with $^{\bullet}OH$.[53]

The specific energy towards TOC removal has been determined in the same manner than with acetaminophen degradation (Eq. 4), by considering C_0 and *C* as the initial TOC concentration and the TOC concentration at time *t* (mg-C L^{-1}), respectively. The evolution of $E_{specific}$ is shown in Fig. 7c. From 45% to 87% of TOC removal, the energy increased from 0.23 to 0.49 kWh g-TOC^{-1}. At similar TOC removal yield (45%), the specific energy in microfluidic reactors was 3.7 times lower than Brillas et al.[34] study. This can be ascribed to the drop of cell potential at very short interelectrode distance, while the transfers are maximized.

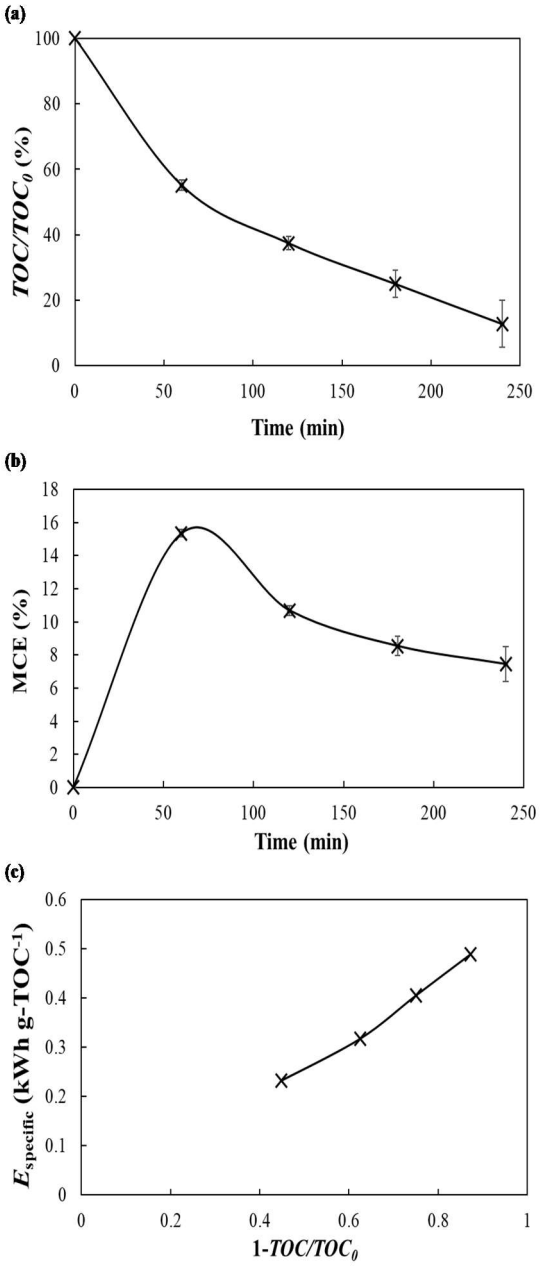

Fig. 7. Influence of reclaimed municipal wastewater on (a) TOC removal yield, (b) current efficiency and (c) specific energy consumption as a function of the pollutant mineralization yield. Operating conditions: $[acetaminophen]_0$ = 0.1 mM, cathode = carbon felt, anode = BDD, interelectrode distance = 500 μm, J_{appl} = 4 mA cm^{-2}, no pH adjustment.

3. Conclusions

This study has shown that a current density of 4 mA cm^{-2} was optimal in BDD-microfluidic electrochemical reactors to degrade acetaminophen in synthetic solution with an optimal interelectrode distance of 500 µm. Since BDD involve heterogeneous oxidation, the reactions should be maximized when the contact between the solution and BDD surface is maximized. This should be the case when the ratio “BDD surface/cell volume” is maximized, i.e. when the interelectrode gap is shorten, until an optimal gap as highlighted in this study. This is explained by the existence of an optimal mass transfer (12.6×10^{-3} m s^{-1}), being reduced at low electrode intervals (from 50 to 250 µm) by the gas bubble generation at the cathode and anode. Nevertheless, the mass transfer was 2 to 10 times higher than in conventional EAOP reactor design. In this condition, the specific energy could be reduced to 0.18 kWh g^{-1} for an 84% acetaminophen decay yield. In addition, an increase of solution conductivity from 0.23 mS cm^{-1} to 2.0 mS cm^{-1} underlined a decrease of energy requirement by 5 times at 85% of pollutant degradation. Nonetheless, the results indicated the possibility of performing electrolysis with a low conductivity solution, such as in a municipal WWTP outlet (1 mS cm^{-1}), without significant loss of disappearance and energy efficiency compared to a solution with a high concentration of supporting electrolyte. Thus, the addition of electrolyte could be avoided, especially in the real wastewater experiments that depicted similar energy efficiency (0.15 kWh g^{-1}) until 60% of pollutant degradation. This is promising for the development of microfluidic electrochemical reactors in such areas. Still, some drawbacks of microfluidic reactor need to be overcome such as their low treatment capacity compared to conventional reactors and their strong ability for clogging. Current research is focusing on this next challenge.

Experimental section

Chemicals

Sulfuric acid (H_2SO_4) was provided by Thermo Fisher Scientific (Karlsruhe, Germany). Acetaminophen was obtained from Sigma-Aldrich (Saint-Quentin-Fallavier, France). Sodium sulfate (Na_2SO_4) was supplied by VWR International (Fontenay-sous-Bois, France). All the chemicals were of analytical grade. Ultrapure water from a Purelab® water purification system (Veolia Water, Antony, France) (resistivity > 18 MΩ cm at room temperature) was used to prepare the solutions.

Synthetic solutions and reclaimed wastewater

In synthetic solutions, H_2SO_4 was supplied to adjust the pH to 3, except in experiments on the influence of electrolyte concentration to avoid the increase of salinity. Although the acidic pH should have no effect on the anodic oxidation experiments,[28] the acidification of solution was performed to compare with future electro-Fenton experiments in which a pH of 3 is necessary to implement Fenton reactions.[1] Na_2SO_4 was added as the supporting electrolyte by varying its concentration from 1 mM to 4 mM and 10 mM, corresponding to solution conductivities of 0.23 mS cm^{-1}, 0.86 mS cm^{-1} and 2.0 mS cm^{-1}, respectively. The reclaimed wastewater was samples at the outlet of a municipal WWTP (Reims, France) and filtered at 0.45 µm before use to avoid the presence of particulate matter. The main physico-chemical characteristics are presented in Table 2. The volume of solution treated with acetaminophen as a representative pollutant (0.1 mM) was 200 mL in synthetic solution and 500 mL in reclaimed wastewater at room temperature (25 ±1 °C).

Electrochemical cell

A flow-by cell was used in a batch recirculated mode using a peristaltic pump (Masterflex l/P, Easy load pump head 77601-10 model, Cole-Parmer, Vernon Hills, IL, USA) at a constant flow rate of 0.43 L min^{-1}. The cell has been manufactured in the laboratory in poly(methyl methacrylate) (PMMA) that is chemically and thermally resistant to the applied conditions. It also allows for visual inspection of the internal reactor such as liquid pathway or gas bubbles

formation. The cathode was a piece of soft graphite felt (RVG 2000 by Mersen, Gennevilliers, France), while the anode was a BDD double side coated (12 µm of layer thickness) on Niobium (Nb) (DiaCCon, Fürth, Germany). The porous felt was embedded in the cathode compartment that has been specifically designed to avoid leakage by connecting the felt with a graphite rod (FINAL Advanced Materials, Rott, France) while the rod was connected with the power supply. This also ensured that no contact between the cathode and anode occurred at very short interelectrode distance. Both the cathode and anode had the same geometric surface area of 50 cm^2 in contact with the solution. The carbon felt was conditioned before use by immersing the material in an ultrasonic bath with an acetone/ultrapure water mixture for 1 h.[54] The material was then thoroughly rinsed with ultrapure water and dried in an oven at 60 °C for 24 h. Each carbon cathode was employed only for one set of experiments to ensure better repeatability of the results. This is to avoid any change of cathode properties after several use (change of porosity, adsorption of organics) and could affect the process efficiency.[42] The interelectrode gap was varied using polytetrafluoroethylene (PTFE) spacers of different thicknesses delivered by Bohlender (Grünsfeld, Germany). The current intensity was applied using a HAMEG 7042-5 (Beauvais, France) power supply, and the current density was calculated as a function of the geometric surface of the BDD anode.

Analytical procedures

Acetaminophen was analyzed with a UV-Vis spectrophotometer (Anthelie Light, Secomam-Aqualabo, Champigny-sur-Marne, France) at a wavelength of 243 nm, giving the maximal absorbance for optimal sensitivity. The amount of acetaminophen could be determined from the calibration curve that gave a molar extinction coefficient of 9767 L mol^{-1} cm^{-1} with an R^2 of 0.9998. Thus, it validated the Beer-Lambert law in the considered range of concentration (0.001-0.1 mM).

A V_{CSH} TC/TN analyzer (Shimadzu; Marne-La-Vallée, France) was employed to quantify the TOC, TIC and TN in reclaimed wastewater.

Ionic chromatography (Dionex/Thermo-Fisher ICS 3000; Noisy-Le-Grand, France) was used to monitor inorganic anion species (NO_2^-, NO_3^-, Cl^-, PO_4^{3-}, SO_4^{2-}) present in reclaimed

wastewater. An AG-19 column guard was connected to an AS-19 anion-exchange column (25 cm × 4 mm) and stored at 30°C. The conductivity detector was heated at 35 °C and the flow rate was set at 1 mL min^{-1}.

A Hach colorimetric method using salicylate procedure and a DR-2400 spectrophotometer (Hach; Lognes, France) were employed to quantify ammonium ions.

Acknowledgments

The authors would like to thank the “Carnot ICEEL” for financial support to “ElectroFil” project.

Keywords: Advanced electro-oxidation • Boron-doped diamond • Interelectrode distance • Mass transfer • Pharmaceutical

References

[1] E. Brillas, I. Sirés, M.A. Oturan, *Chem. Rev.* **2009**, 109, 6570–6631.

[2] I. Sirés, E. Brillas, M.A. Oturan, M.A. Rodrigo, M. Panizza, *Environ. Sci. Pollut. Res.* **2014**, 21, 8336–8367.

[3] M.A. Rodrigo, N. Oturan, M.A. Oturan, *Chem. Rev.* **2014**, 114, 8720–8745.

[4] C.A. Martínez-Huitle, M.A. Rodrigo, I. Sirés, O. Scialdone, *Chem. Rev.* **2015**, 115, 13362–13407.

[5] F.C. Moreira, R.A.R. Boaventura, E. Brillas, V.J.P. Vilar, *Appl. Catal. B Environ.* **2017**, 202, 217–261.

[6] B.P. Chaplin, *Environ. Sci. Process. Impacts*. **2014**, 16, 1182–203.

[7] E. Mousset, N. Oturan, M.A. Oturan, *Appl. Catal. B Environ.* **2018**, 226, 135–146.

[8] M.A. Oturan, *J. Appl. Electrochem.* **2000**, 30, 475–482.

[9] M. Panizza, G. Cerisola, *Chem. Rev.* **2009**, 109, 6541–6569.

[10] C.A. Martínez-Huitle, M. Panizza, *Curr. Opin. Electrochem.* **2018**, 11, 62-71.

[11] E. Brillas, C.A. Martínez-Huitle, *Appl. Catal. B Environ.* **2015**, 166–167, 603–643.

[12] M. Panizza, E. Brillas, C. Comninellis, *J. Environ. Eng. Manag.* **2008**, 18, 139–153.

[13] M. Panizza, P.A. Michaud, G. Cerisola, C. Comninellis, *J. Electroanal. Chem.* **2001**, 507, 206–214.

[14] P.V. Nidheesh, G. Divyapriya, N. Oturan, C. Trellu, M.A. Oturan, *ChemElectroChem* **2019**, 6, 1-20.

[15] O. Scialdone, C. Guarisco, A. Galia, G. Filardo, G. Silvestri, C. Amatore, C. Sella, L. Thouin, *J. Electroanal. Chem.* **2010**, 638, 293–296.

[16] O. Scialdone, A. Galia, S. Sabatino, *Appl. Catal. B Environ.* **2014**, 148–149, 473–483.

[17] O. Scialdone, A. Galia, S. Sabatino, *Electrochem. Commun.* **2013**, 26, 45–47.

[18] J.F. Pérez, J. Llanos, C. Sáez, C. López, P. Cañizares, M.A. Rodrigo, *Electrochem. Commun.* **2017**, 82, 85–88.

[19] E. Mousset, Y. Pechaud, N. Oturan, M.A. Oturan, *Appl. Catal. B Environ.* **2019**, 240, 102–111.

[20] B. Lopez, P. Ollivier, A. Togola, N. Baran, J.P. Ghestem, *Sci. Total Environ.* **2015**, 518–

519, 562–573.

[21] L. Kong, K. Kadokami, S. Wang, H.T. Duong, H.T.C. Chau, *Chemosphere*. **2015**, 122, 125–130.

[22] D. Simazaki, R. Kubota, T. Suzuki, M. Akiba, T. Nishimura, S. Kunikane, *Water Res.* **2015**, 76, 187–200.

[23] S. Periyasamy, M. Muthuchamy, *J. Environ. Chem. Eng.* **2018**, 6, 7358–7367.

[24] S.D. Richardson, S.Y. Kimura, *Anal. Chem.* **2016**, 88, 546–582.

[25] E. Mousset, L. Frunzo, G. Esposito, E.D. van Hullebusch, N. Oturan, M.A. Oturan, *Appl. Catal. B Environ.* **2016**, 180, 189–198.

[26] E. Mousset, N. Oturan, E.D. van Hullebusch, G. Guibaud, G. Esposito, M.A. Oturan, *Appl. Catal. B Environ.* **2014**, 160–161, 666–675.

[27] F. Sopaj, N. Oturan, J. Pinson, F. Podvorica, M.A. Oturan, *Appl. Catal. B Environ.* **2016**, 199, 331–341.

[28] E. Brillas, I. Sirés, C. Arias, P. Cabot, F. Cantellas, R.M. Rodriguez, J.A. Garrido, *Chemosphere*. **2005**, 58, 399–406.

[29] P. Cañizares, R. Paz, C. Sáez, M.A. Rodrigo, *J. Environ. Manage.* **2009**, 90, 410–420.

[30] A. Kapałka, G. Fóti, C. Comninellis, *J. Appl. Electrochem.* **2008**, 38, 7–16.

[31] M. Panizza, P.A. Michaud, G. Cerisola, C. Comninellis, *Electrochem. Commun.* **2001**, 3, 336–339.

[32] P. Cañizares, I.F. De Marcos, M.A. Rodrigo, J. Lobato, *J. Chem. E*. **2006**, 83, 1204–1207.

[33] H. Olvera-Vargas, J.C. Rouch, C. Coetsier, M. Cretin, C. Causserand, *Sep. Purif. Technol.* **2018**, 203, 143–151.

[34] E. Brillas, I. Sirés, C. Arias, P.L. Cabot, F. Centellas, R.M. Rodríguez, J.A. Garrido, *Chemosphere*. **2005**, 58, 399–406.

[35] A. Anglada, A.M. Urtiaga, I. Ortiz, *J. Hazard. Mater.* **2010**, 181, 729–35.

[36] O. Scialdone, A. Galia, S. Sabatino, G.M. Vaiana, D. Agro, A. Busacca, C. Amatore, *ChemElectroChem*. **2014**, 1, 116–124.

[37] J. Křišťál, R. Kodým, K. Bouzek, V. Jiřičný, *Electrochem. Commun.* **2008**, 10, 204–207.

[38] E.V. dos Santos, S.F.M. Sena, D.R. da Silva, S. Ferro, A. De Battisti, C.A. Martínez-Huitle, *Environ. Sci. Pollut. Res.* **2014**, 21, 8466–8475.

[39] C. Trellu, B.P. Chaplin, C. Coetsier, R. Esmilaire, S. Cerneaux, C. Causserand, M. Cretin, *Chemosphere*. **2018**, 208, 159–175.

[40] J.H.B. Rocha, A.M.S. Solano, N.S. Fernandes, D.R. da Silva, J.M. Peralta-Hernandez, C.A. Martínez-Huitle, *Electrocatalysis*. **2012**, 3, 1–12.

[41] O. Scialdone, C. Guarisco, A. Galia, *Electrochim. Acta*. **2011**, 58, 463–473.

[42] E. Mousset, S. Pontvianne, M.-N. Pons, *Chemosphere*. **2018**, 201, 6–12.

[43] J. Davis, J.C. Baygents, J. Farrell, *Electrochim. Acta*. **2014**, 150, 68–74.

[44] K. Serrano, P.A. Michaud, C. Comninellis, A. Savall, *Electrochim. Acta*. **2002**, 48, 431–436.

[45] E. Mousset, V. Huang Weiqi, B. Foong Yang Kai, J.S. Koh, J.W. Tng, Z. Wang, O. Lefebvre, *J. Mater. Chem. A*. **2017**, 5, 24951–24964.

[46] E. Mousset, Z. Wang, O. Lefebvre, *Water Sci. Technol.* **2016**, 74, 2068–2074.

[47] N. Barhoumi, H. Olvera-Vargas, N. Oturan, D. Huguenot, A. Gadri, S. Ammar, E. Brillas, M.A. Oturan, *Appl. Catal. B Environ.* **2017**, 209, 637–647.

[48] B. Garza-Campos, E. Brillas, A. Hernandez-Ramirez, A. El-Ghenymy, J.L. Guzman-Mar, E.J. Ruiz-Ruiz, *J. Hazard. Mater.* **2016**, 319, 34–42.

[49] C. Trellu, S. Chakraborty, P.V. Nidheesh, M.A. Oturan, *ChemElectroChem* **2019**, 6, 1-15.

[50] E. Lacasa, J. Llanos, P. Cañizares, M.A. Rodrigo, *Chem. Eng. J.* **2012**, 184, 66–71.

[51] Y. Lan, C. Coetsier, C. Causserand, K. Groenen Serrano, *Electrochim. Acta*. **2017**, 231, 309–318.

[52] G. V. Buxton, A.J. Elliot, *Int. J. Radiat. Appl. Instrumentation. Part C*. **1986**, 27, 241–243.

[53] C. Trellu, Y. Péchaud, N. Oturan, E. Mousset, D. Huguenot, E.D. van Hullebusch, G. Esposito, M.A. Oturan, *Appl. Catal. B Environ.* **2016**, 194, 32–41.

[54] T.X.H. Le, C. Charmette, M. Bechelany, M. Cretin, *Electrochim. Acta*. **2016**, 188, 378–384.